Effect of Ca Addition on the Corrosion Resistance of Gravity Cast AZ31 Magnesium Alloy

Chang Dong Yim, Young Min Kim and Bong Sun You

Energy Materials Research Center, Korea Institute of Machinery and Materials,
Sangnam 66, Changwon, Gyeongnam 641-831, Korea

The effect of Ca addition on the corrosion resistance of AZ31 magnesium alloys was evaluated by observation of microstructure and measurement of corrosion potential and average corrosion rate. The main mechanism of corrosion of AZ31+xCa ($x = 0 \sim 5$ mass%) alloys was galvanic-corrosion between α-Mg and second phase. But the propagation behavior of corrosion was different with Ca content. In the alloy containing below 0.7 mass%Ca, a micro-galvanic cell formed between matrix α-Mg and second phase formed semi-continuously at grain boundaries and the corrosion progressed in transgranular mode. The propagation of corrosion was retarded when the corrosion front met the second phase acted as corrosion barrier. But in the alloys containing above 1 mass%Ca, a micro-galvanic cell formed between eutectic α-Mg and discontinuous second phase in the eutectic region and the corrosion rapidly progressed along eutectic α-Mg formed continuously at grain boundaries because the discontinuous second phase could not prohibit the propagation of corrosion effectively.
[doi:10.2320/matertrans.48.1023]

1. Introduction

Nowadays the magnesium alloys are being widely applied to structural parts, especially automotive and mobile electronic parts due to high specific strength/stiffness, good castability and excellent vibration/shock absorption ability.[1–4] However, the magnesium alloys are currently still not as popular as aluminum alloys due to low ultimate tensile strength, poor corrosion resistance and formability at room temperature. Magnesium and magnesium alloys can suffer a number of different forms of corrosion such galvanic, intergranular and localized corrosion.[5] In general, the magnesium alloys are highly susceptible to galvanic corrosion. Galvanic corrosion is usually observed as heavy localized corrosion of the magnesium adjacent to the cathode.[6] Cathodes can be external as other metals in contact with magnesium, or may be internal as second or impurity phases. The galvanic corrosion rate is increased by high conductivity of the medium, large potential difference between anode and cathode, low polarisability of anode and cathode, large area ratio of cathode to anode, and small distance from anode to cathode.[7] Magnesium and magnesium alloys are virtually immune to intercrystalline attack.[8] Corrosion does not penetrate inwards along the grain boundaries,[9] because the grain-boundary phases are invariably cathodic to the grain interior.[8] Magnesium is a naturally passive metal that undergoes pitting corrosion at its free corrosion potential, E_{corr}, when exposed to chloride ions in a non-oxidizing medium.[10] As a result the corrosion of magnesium alloys in neural or alkaline salt solutions typically takes the form of pitting. Heavy metal contamination promotes general pitting attack. In Mg-Al alloy, pits are often formed due to selective attack along the $Mg_{17}Al_{12}$ network which is followed by the undercutting and falling out of grains.[6] These major corrosion of magnesium alloys are caused by the change of microstructural factors, especially morphology and volume fraction of second phases formed at grain boundaries, when the alloying elements are added to the magnesium alloys.

Ca is very promising element because the addition of Ca significantly improves the high temperature strength and creep resistance[11–13] and it has low density and is low cost. Ca is also very effective for improving the ignition resistance of molten magnesium alloys,[14,15] which stimulated the development of non-combustible magnesium alloys. Magnesium and its alloys are very active in molten state and rapidly ignited or combusted when the clean surface of melt is in contact with oxygen in air. So, in general, protecting gas consisted of SF_6, CO_2 and air is blown to melt surface during melting and casting operation. But SF_6 is the strongest one of greenhouse gases which cause global warming. In near future, the usage of SF_6 will be prohibited strictly, which motivates the R & D for new melt protection methods. There are two major melt protection techniques to be developed. One is improvement of ignition resistance of molten magnesium alloys by addition of alloying elements[16–19] and the other is using other gas such as SO_2 and HFC-134a.[20,21] The method of addition of alloying elements has several advantages compared to using protection gas. There is no need for gas blowing equipment, which gives more freedom to designs of process and manufacturing equipment. The inherent ignition resistance of magnesium alloys increases, which makes a possibility of burning of various parts lower. As mentioned above, the ignition resistance of alloys containing Ca in molten state increases with increasing of Ca content. The addition of Ca changes not only the ignition resistance of melt but also the various properties such as tensile strength, elongation and corrosion resistance, etc. There have been many studies about the effects of Ca on ignition resistance and mechanical properties.[14–23] Although the corrosion resistance is one of important factors in aspects of application, there is little study about the corrosion behavior of magnesium alloys containing Ca. In this study, the effect of Ca on corrosion resistance of gravity cast AZ31+xCa alloys containing $0 \sim 5$ mass%Ca was investigated experimentally and analyzed in aspects of microstructural

Table 1   Chemical compositions of gravity cast AZ31+xCa alloys (mass%).

Alloys	Al	Zn	Mn	Ca	Mg
AZ31	3.20	0.92	0.13	—	Bal.
AZ31-0.3Ca	2.97	0.95	0.42	0.31	Bal.
AZ31-0.5Ca	2.91	0.92	0.42	0.49	Bal.
AZ31-0.7Ca	2.77	0.94	0.42	0.72	Bal.
AZ31-1.0Ca	2.89	0.75	0.44	1.03	Bal.
AZ31-2.0Ca	3.07	0.73	0.43	2.11	Bal.
AZ31-5.0Ca	2.90	0.68	0.42	5.10	Bal.

change by means of observation of microstructure and measurement of corrosion potential and average corrosion rate.

2. Experimental Procedure

AZ31B ingot of 3 kg was inserted into a low carbon steel crucible and heated to 923 K. Protecting gas consisted of $SF_6 : CO_2 = 1 : 10$ was blown into the crucible at flow rate of 5 ml/s to prevent the ignition and/or combustion of melt. After the AZ31B ingot was melted completely, Ca pellet of 9~150 g was added into the melt and heated up 993 K. The melts was isothermally held at 993 K for 30 minutes for Ca to be dissolved completely. A vacuum treatment was carried out to make the non-metallic inclusions floated to melt surface and non-metallic inclusions was removed by using a skimmer before casting. A gravity casting was produced by pouring the melt into a plate-type mold preheated to 573 K. Table 1 shows the alloy compositions analyzed by inductively coupled plasma (ICP) spectrometer.

Specimens were cut into a proper size from gravity casting of AZ31+xCa alloys and mounted by using polymer resin. The specimens were mechanically polished by using emery papers of #100~2400 and pastes containing diamond particles of 1 μm diameter and then etched by using acetic picral solution (10 mL acetic acid + 4.2 g picric acid + 10 mL distilled water + 70 mL ethanol (95%)) in order to reveal the microstructure more distinctly. The microstructures of gravity cast AZ31+xCa alloys were observed by using an optical microscope and a scanning electron microscope.

Electrochemical polarization tests were carried out using Princeton Applied Research Versa Stat. II to measure the corrosion potentials of gravity cast AZ31+xCa alloys and Mg+xCa alloys. Working electrodes were prepared by connecting a wire to one side of the sample and covering with cold resin. The opposite surface of the specimen was exposed to the solution. The exposed area was about 0.5 cm^2. The specimens were mechanically polished prior to each test, followed by washing with acetone. A polarization test was carried out in a corrosion cell containing 1000 mL of 3.5 mass%NaCl solution using a standard three electrode configuration: Ag/AgCl as reference electrode with a carbon electrode as counter and the sample as the working electrode. Specimens were immersed in the test solution and a polarization scan was carried out toward more noble value at a rate of 1 mV s^{-1} for 3.6 ks. The corrosion potential was defined as the value stabilized after immersion for 3.6 ks.

A constant immersion test was carried out to evaluate the effect of Ca on the average corrosion rate of AZ31+xCa

alloys. Sample preparation and immersion test were done in according to the procedure of ASTM standard G-31-72.[24] The mechanically polished and preweighed specimens were exposed to the 5 mass%NaCl solution for 4320 ks. Final cleaning of the specimen at the end of the test was carried out by dipping it in a chromic acid solution (200 g CrO$_3$ + 10 g AgNO$_3$ + 1000 mL distilled water) at boiling condition followed by acetone washing. The weight loss was measured after each test and the corrosion rate was calculated in mills per year.

3. Results and Discussion

Figure 1 shows the microstructures of gravity cast AZ31+xCa alloys with Ca content. The average size of α-Mg grain decreased with increasing Ca content, which was resulted from slow diffusion of solute Ca. The solute discharged from liquid during solidification is accumulated in front of solid/liquid interface because of slow diffusion of solute. So constitutional undercooling is generated in a diffusion layer ahead of the advancing solid/liquid interface, which restricts the grain growth.[25] In addition, further nucleation occurs in front of the interface because nucleants in the melt are more likely to survive and be activated in the constitutionally undercooled zone. The area of interdendritic region also increased with increasing Ca content.

Figure 2 shows the SEM photographs of AZ31+xCa alloys with Ca content. In the alloys containing below 0.7 mass%Ca, the eutectic regions were not observed distinctly and a second phase formed semi-continuously along grain boundaries of α-Mg phase. As the calcium content increased above 1 mass%, eutectic regions with fine lamellar structure were observed along grain boundaries. The volume fraction of eutectic region increased with increasing of Ca and in the alloy containing 5 mass%Ca, most of intergranular region between α-Mg grains was consisted of eutectic phase.

Figure 3 shows the corrosion properties of gravity cast AZ31+xCa alloys as function of Ca content. The corrosion resistance of AZ31+xCa alloys increased with Ca content up to $x = 0.7$, but decreased remarkably above 1 mass%Ca. Figure 4 shows the vertical section of AZ31+xCa alloy specimens after immersion test. In the alloys containing below 0.7 mass%Ca, the alloys were attacked homogeneously by corrosion. It seemed that the corrosion front was arrested by the second phase formed semi-continuously along grain boundaries of α-Mg phase. On the other hand, it seemed that the corrosion was initiated locally and typical pitting was observed in the alloys containing above 1 mass%Ca. As shown in Fig. 4(c), the corrosion propagated along grain boundary. The eutectic region between α-Mg grains was attacked preferentially by corrosion as shown in Fig. 4(e). This difference of corrosion resistance with Ca content was mainly resulted from change of morphology of second phase. When the second phase formed along grain boundary and the volume fraction of second phase is low as shown in Fig. 3(a) and Fig. 5(a), the corrosion is initiated at matrix α-Mg phase near second phase due to formation of internal microgalvanic cell. The corrosion front does not penetrate the second phase because the second phase is invariably cathodic to the grain interior.[8] So the corrosion propagates through
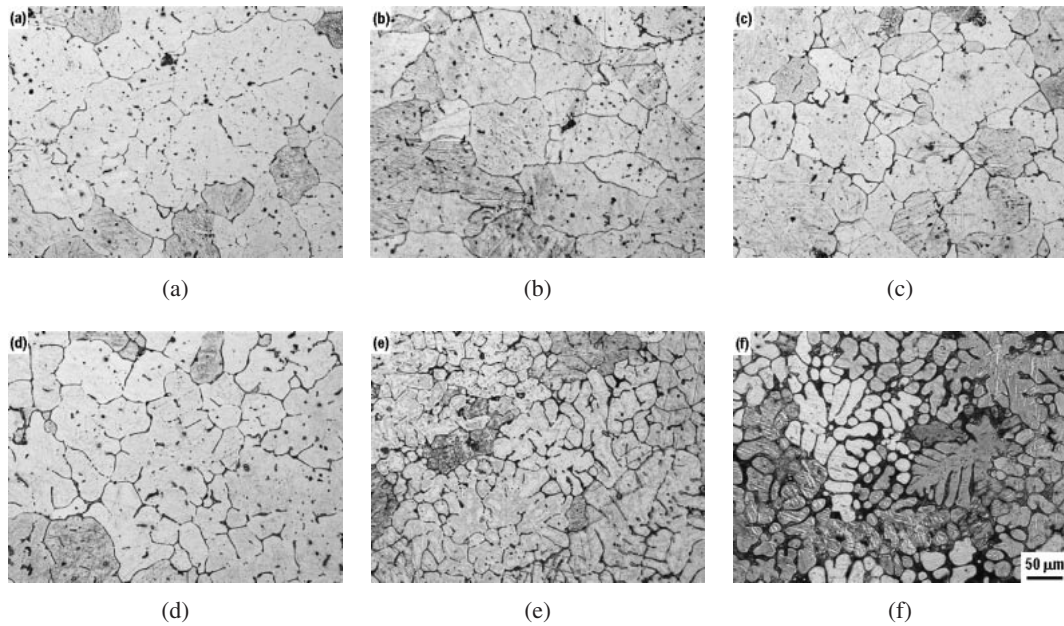
Fig. 1   Microstructures of gravity cast AZ31+xCa alloys with Ca content; (a) $x = 0.3$ (b) $x = 0.5$ (c) $x = 0.7$ (d) $x = 1.0$ (e) $x = 2.0$ (f) $x = 5.0$.
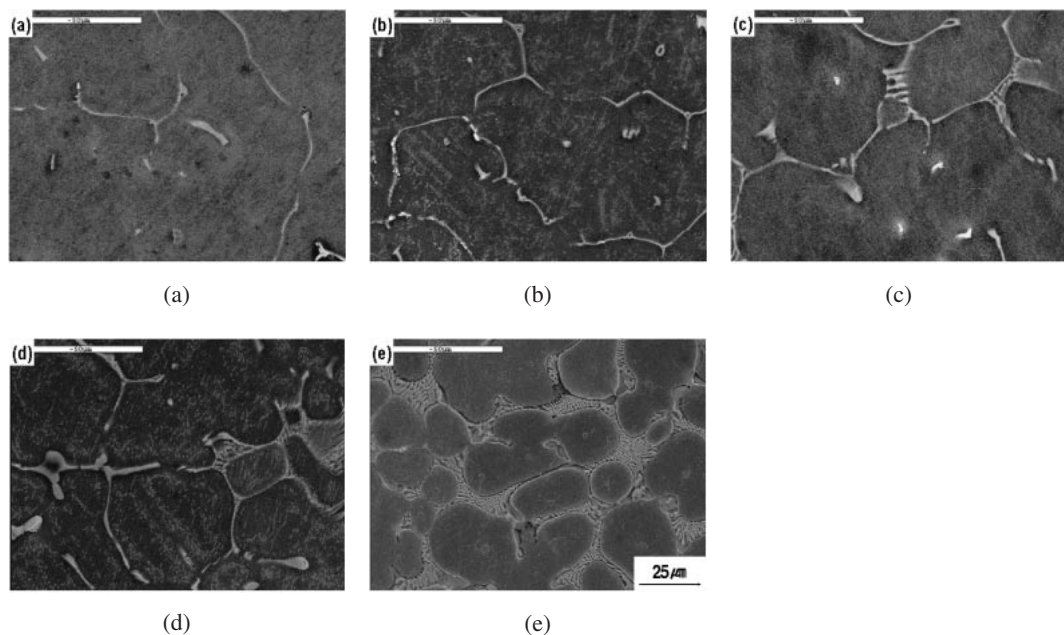

Fig. 2   SEM photographs of gravity cast AZ31+xCa alloys with Ca content; (a) $x = 0.5$ (b) $x = 0.7$ (c) $x = 1.0$ (d) $x = 2.0$ (e) $x = 5.0$.

matrix α-Mg phase and the corrosion fronts from different grains meet together as the corrosion proceeds. At this time, the discontinuous second phase is undercut by connection of corrosion fronts as shown in Fig. 5(a) and so the corrosion is not retarded effectively by second phase. When the second phase formed along grain boundary and the volume fraction of second phase is high enough to enclose the α-Mg grain as shown in Fig. 3(b) and Fig. 5(b), the corrosion is also initiated at matrix α-Mg phase near second phase and propagates through matrix α-Mg phase. But the corrosion fronts from the neighboring grains don't meet together by the second phase formed semi-continuously along grain boundaries and the corrosion is arrested at grain boundaries. In the

alloys containing above 1 mass%Ca, the eutectic structure consisted of eutectic α-Mg and intermetallic second phases formed in the interdendritic region as shown in Fig. 3(c)–(e). The internal micro-galvanic cell is formed between eutectic α-Mg and second phase in interdendritic region. So the corrosion is initiated at eutectic α-Mg phase and propagates fast along eutectic α-Mg phase formed continuously along grain boundary as shown in Fig. 5(c). At this time, the discontinuous second phase in interdendritic region can not interrupt the propagation of corrosion effectively, which results in lower corrosion resistance.

The internal galvanic corrosion is also affected by the potential difference between anodic and cathodic phases. The
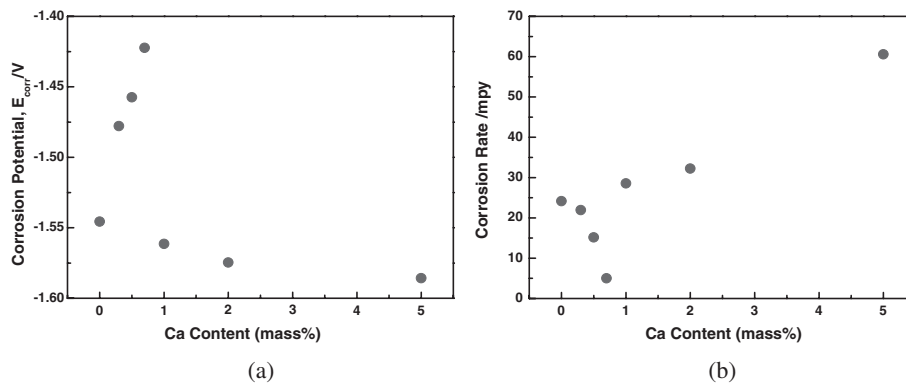
Fig. 3　Corrosion properties of gravity cast AZ31+xCa alloys; (a) corrosion potential (b) average corrosion rate.

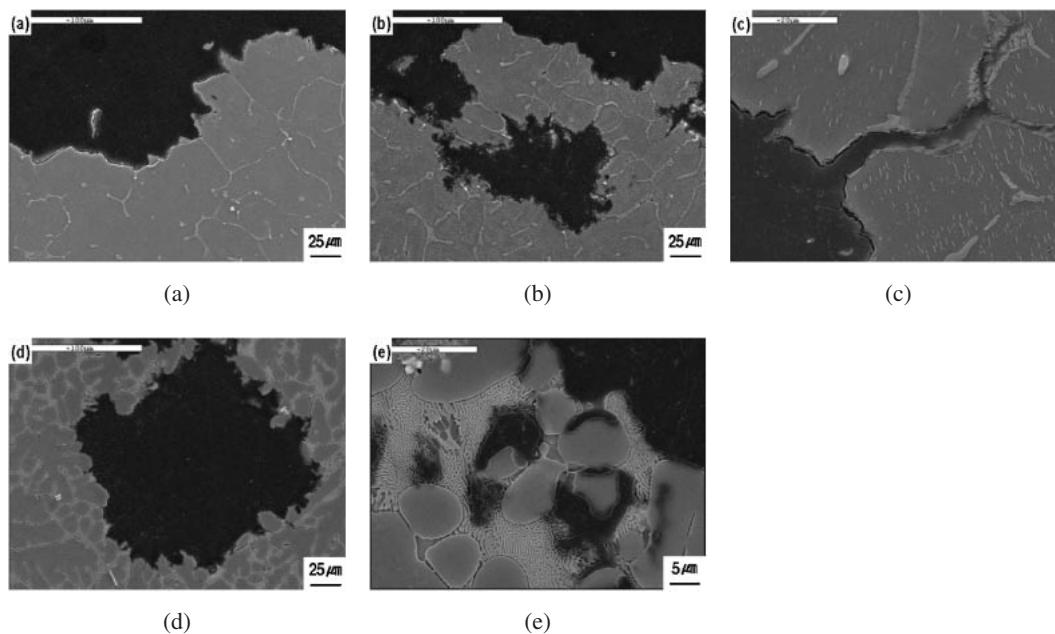(a)　　　　　　　　　　　　　(b)　　　　　　　　　　　　　(c)

(d)　　　　　　　　　　　　　(e)

Fig. 4　Vertical-sectional view of AZ31+xCa alloy specimens after immersion test: (a) $x = 0.7$, (b) and (c) $x = 2.0$ (d) and (e) $x = 5.0$.

corrosion potential of matrix α-Mg phase would change by addition of Ca because some of Ca added into AZ31 magnesium alloy would be solutionized into α-Mg phase during solidification. Figure 6 shows the change of Ca content in matrix α-Mg phase calculated by using Thermocalc in Scheil mode. Although the maximum solubility of Ca in α-Mg phase is 1.34 mass%, only 0.7 mass%Ca was dissolved into α-Mg phase during solidification because of slow diffusion of solute Ca. Based on this calculation, the corrosion potentials of Mg+xCa binary alloys ($x = 0$–0.7 mass%) were measured as shown in Fig. 7. The Mg-xCa alloys were produced by gravity casting and a solid solution heat treatment was carried out for solute Ca to be dissolved completely into α-Mg phase and minimize the concentration gradient. As shown in Fig. 7, the corrosion potentials of Mg-xCa alloys with single α-Mg phase increased with increasing the Ca content. So the potential difference between matrix α-Mg phase and second phase would decrease with increasing the Ca content, which resulted in higher corrosion resistance.

The addition of Ca into AZ31 magnesium alloy changes the species of second phase as well as the corrosion potential

of matrix α-Mg phase. In the alloys containing below 0.7 mass%Ca, (Mg,Al)$_2$Ca phase with Laves C35 structure was mainly observed. As Ca content increased, Mg$_2$Ca phase with Laves C14 structure was observed and in the alloys 5 mass%Ca, most of intermetallic compounds observed at grain boundaries were Mg$_2$Ca phase. This change of intermetallic compounds with Ca content is coincided with the previous study.[26] The corrosion potential of second phase could not be measured exactly because of the difficulty in separate production of second phase. In this study, it was assumed that the potential difference between (Mg,Al)$_2$Ca and Mg$_2$Ca phases would be little due to similarity of crystal structures of both phases. So the change of second phase with Ca content from (Mg,Al)$_2$Ca phase to Mg$_2$Ca phase would not affect the internal galvanic corrosion.

4.　Conclusion

The corrosion resistance of gravity cast AZ31+xCa alloys was strongly dependent on the morphology of second phase. In the alloys containing below 0.7 mass%Ca, a micro-
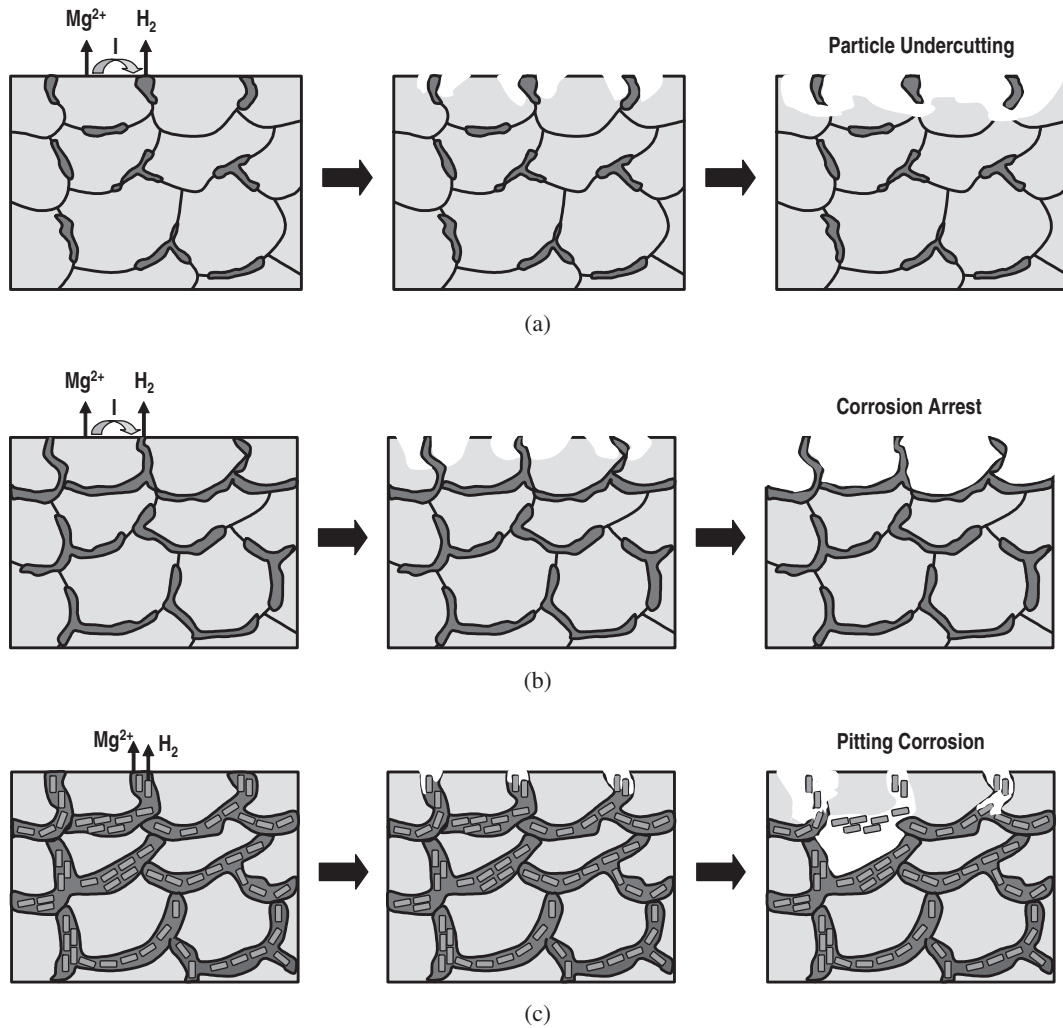
Fig. 5   Internal galvanic corrosion of magnesium alloy; (a) discontinuous second phase at grain boundary (b) semi-continuous second phase at grain boundary (c) discontinuous second phase in eutectic region.
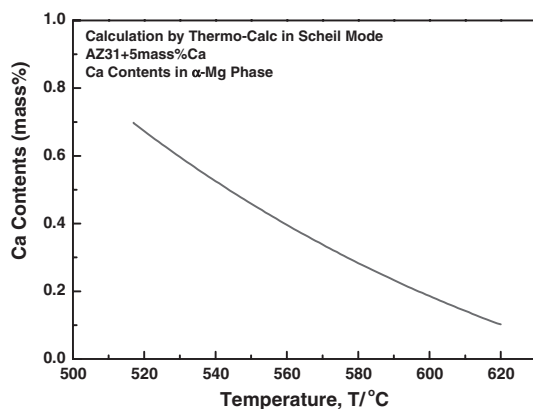

Fig. 6   Change of Ca content in α-Mg phase during solidification of AZ31+5 mass%Ca alloy.
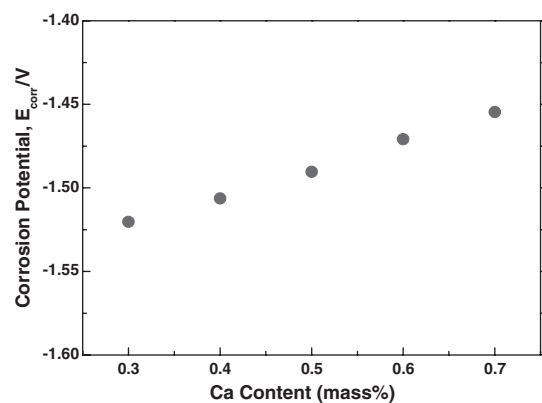
Fig. 7   Change of corrosion potentials of Mg+xCa alloys with Ca content.

galvanic cell would form between the matrix α-Mg phase and the second phase formed semi-continuously at grain boundaries. The corrosion was initiated at α-Mg phase near second phase and propagated through α-Mg phase. At low volume fraction of second phase, the second phase did not envelop α-Mg phase completely. So the second phases were undercut by connection of corrosion fronts from neighboring grains and did not act as effective corrosion barrier. But in the case of high volume fraction of second phase, the second phase surrounded α-Mg phase nearly. So the corrosion was retarded when the corrosion front met the second phase at grain boundary, which resulted in higher corrosion resistance. In the alloys containing above 1 mass%Ca, a micro-

galvanic cell would form between the eutectic α-Mg phase and discontinuous second phase at interdendritic region. The corrosion was initiated at the eutectic α-Mg phase and propagated fast through eutectic α-Mg phase. The discontinuous second phase in the eutectic region did not interrupt the propagation of corrosion effectively. With increasing of Ca content, the area fraction of eutectic region increased and the corrosion was propagated faster. The increase of corrosion potential of matrix α-Mg phase by addition of Ca also contributed to the improvement of corrosion resistance. The difference of corrosion potential between α-Mg phase and second phase decreased by increasing of corrosion potential of α-Mg phase, which resulted in slow propagation of corrosion.

Acknowledgement

REFERENCES

1) H. Hu, A. Yu, N. Li and J. E. Allison: Mater. Manufacturing Processes **18** (2003) 687–717.
2) A. A. Luo: Inter. Mater. Rev. **49** (2004) 13–30.
3) L. Lin, Z. Liu, L. Chen, T. Liu and S. Wu: Met. Mater. Inter. **10** (2004) 501–507.
4) J. C. Benedyk: Light Metal Age **63** (2005) 36–38.
5) G. L. Song and A. Atrens: Adv. Eng. Mater. **1** (1999) 11–33.
6) A. Froats, T. K. Aune, D. Hawke, W. Unsworth and J. Hills: *Metals Handbook*, 9th ed., vol. 13, (ASM International, Materials Park, OH, 1987) pp. 740–754.
7) W. S. Loose: *Corrosion and Protection of Magnesium*, (ASM International, Materials Park, OH, 1946) pp. 173–180.
8) G. L. Makar and J. Kruger: Inter. Mater. Rev. **38** (1993) 138–153.
9) E. F. Emley: *Principles of Magnesium Technology*, (Pergamon Press, New York, 1966) pp. 670–688.
10) R. Tunold, H. Holtan, M. B. Hagg Berfe, A. Lasson and R. Steen-Hansen: Corr. Sci. **17** (1977) 353–365.
11) R. Ninomiya, T. Ojiro and K. Kubota: Acta Metall. Mater. **43** (1995) 669–674.
12) Y. Terada, R. Sota, N. Ishimatsu, T. Sato and K. Ohori: Metall. Mater. Trans. A **35** (2004) 3029–3032.
13) B. R. Powell, A. A. Luo, V. Rezhets and B. L. Tiwari: J. Mater. Manufacturing **110** (2001) 406–410.
14) B. S. You, W. W. Park and I. S. Chung: Scripta mater. **42** (2000) 1089–1094.
15) B. H. Choi, B. S. You and I. M. Park: Met. Mater. Inter. **12** (2006) 63–68.
16) M. Sakamoto, S. Akiyama, T. Hagio and K. Ogi: J. Jpn. Foundry Eng. Soc. **69** (1997) 227–233.
17) S. Y. Chang and J. C. Choi: Met. Mater. Inter. **4** (1998) 165–172.
18) M. H. Kim, W. W. Park, B. S. You, Y. B. Huang and W. C. Kim: Mater. Sci. Forum **419–422** (2003) 575–580.
19) Y. B. Huang, I. S. Chung, B. S. You, W. W. Park and B. H. Choi: Met. Mater. Inter. **10** (2004) 7–12.
20) S. Cashion and N. Ricketts: *Magnesium Technology 2000*, ed. by H. I. Kaplan, J. N. Hryn and B. B. Clow, (TMS, 2000) pp. 77–81.
21) N. Ricketts and S. Cashion: *Magnesium Technology 2001*, ed. by J. N. Hryn, (TMS, 2001) pp. 31–36.
22) B. H. Choi, B. S. You, C. D. Yim, W. W. Park and I. M. Park: Mater. Sci. Forum **475–479** (2005) 2477–2480.
23) W. Qudong, L. Yizhen, Z. Xiaoqin, D. Wenjiang, Z. Yanping, L. Qinghua and L. Jie: Mater. Sci. Eng. A **271** (1999) 109–115.
24) *Annual Book of ASTM Standards Parts 3 and 4*, (ASTM, 1972) pp. 552–559.
25) Y. C. Lee, A. K. Dahle and D. H. StJohn: Metall. Mater. Trans. A **31** (2000) 2895–2906.
26) A. Suzuki, N. D. Saddock, J. W. Jones and T. M. Pollock: Acta mater. **53** (2005) 2823–2834.